

# Tensile Shear Strength of Steel Plate-reinforced Larch Timber as Affected by Further Reinforcement of the Wood with Carbon Fiber Reinforced Polymer (CFRP)

In-Hwan Lee, Yo-Jin Song, and Soon-Il Hong \*

To improve the connecting strength of larch timbers, tensile shear test specimens were fabricated, and their connecting shear strength performance was examined. The control specimens consisted of larch timber reinforced with steel plate. These were compared with similar specimens in which the wood had been reinforced with carbon fiber reinforced polymer (CFRP). The reinforced specimens were fabricated in three types depending on the position of the CFRP reinforcement in the wooden part. All specimens were fabricated in two end distance types, depending on the bolt insertion position. The end distances examined were 60 mm (5D) and 84 mm (7D). The maximum connecting strength and the yield shear strength of each type were not different according to the CFRP reinforcement position. The reinforced specimens had an average connecting strength and yield shear strength that was 24% to 29% higher than the control specimens. The CFRP-reinforced specimens with an end distance of 5D had an average connecting strength and an average yield shear strength that was 70% and 26% higher, respectively, than non-reinforced 7D specimens. The yield shear strength was predicted by measuring the bearing strengths of the larch timber samples and CFRP-reinforced timber samples. The predicted yield shear strength matched the measured yield shear strength.

*Keywords:* CFRP; FRP; GFRP; Reinforced; FRP-reinforced timber; Tensile shear strength; Timber-steel plate-timber; Yield shear strength

*Contact information:* College of Forest & Environmental Sciences, Kangwon National University, 1, kangwondaehak-gil, ChunCheon-si, Gangwon-do, 24341, Republic of Korea;

\* Corresponding author: hongsi@kangwon.ac.kr

## INTRODUCTION

The column-beam connections of heavy-wood structure buildings require high strength characteristics because they receive various loads simultaneously (Song *et al.* 2019). These loads include axial load, lateral load transmitted between both ends of the members, lateral moment, and torsional moment. Generally, the mortise and tenon joint method, the steel-plate-insert method, or the steel-plate-side-member-type connecting method using steel plates are used for the connections of heavy-wood structures (Gečys and Daniūnas 2013; Lee *et al.* 2016; Lee *et al.* 2017). The mortise and tenon joint method can cause residual deformation and initial slipping, requires processing precision, and has a complex structural analysis and design process. Moreover, it is difficult to predict the stiffness and structural stability of the connection using this method due to the low contact force between the members. The excellent strength performance of the connections using steel plates has been verified through various studies (Kim 2005; Xu *et al.* 2009).

The steel plate side members can be joined to a wooden member by drilling holes, but because the joining hardware is exposed to the outside air, there is a high risk of corrosion and a poor appearance. By contrast, the steel plate insert type has excellent aesthetics, although it requires precise prior slit processing. The pre-cut machining technique was recently commercialized, and research has been conducted on steel-plate-insert-type connections (Barber 2017; Le and Tsai 2019). The steel-plate-insert-type connection is formed by joining it with wooden materials using fasteners such as drift pins or bolts. For connections joined by fasteners, it is essential to secure the end distance. Thus, if the end distance is reduced by reinforcement, the design freedom will improve.

Partial reinforcement of the connections can achieve a higher reinforcement effect relative to the reinforcement than the method of reinforcing all the members. Partially reinforced connections also have a relatively small volume and weight. Barber reported that timber and steel-plate-insert-type connections can effectively transmit the force acting on the members and can secure aesthetics. Haller and Wehsener (2000) reported that the connecting strength of the fiber-reinforced wooden connection is up to twice as high as that of the non-reinforced connection. Kim *et al.* (2008) conducted a tensile shear test to examine the bolt connection shear performance of reinforced larch glulam according to the fabric-type fiberglass combination. The test results showed that the yield shear strength of the fabric-type fiberglass-reinforced glulam in the 12-mm-diameter bolt connection was approximately 22% higher than that of the non-reinforced connection, and approximately 20% higher than that of the 16-mm-diameter bolt connection.

Because connections made of timber have a greater variability than the glulam that is laminated after defect removal, it is expected that reinforcing such connections will reduce the strength deviation and improve the connecting strength (Lee *et al.* 2017, 2018). The strength performance of wooden connections can vary depending on the reinforcement combination. The research on connections generally focuses on the reinforcement type or connecting performance, and the evaluation of the strength performance according to the reinforcement combination that needs to be performed.

In this study, steel-plate-insert-type connections made of larch timber and steel-plate-insert-type connections reinforced with carbon-fiber-reinforced plastic (CFRP) were fabricated, and their tensile shear strengths were examined. Different types of specimens were fabricated according to the CFRP reinforcement position and with the 60 mm (5D) and 84 mm (7D) end distances. In addition, the yield shear strength was predicted by measuring the bearing strengths of the larch timber and the CFRP-reinforced timber samples.

## EXPERIMENTAL

### Material

Domestic larch timbers (*Larix kaempferi* Carr.) with an average air-dried water content of 16%, an average air-dried specific gravity of 0.52 g/cm<sup>3</sup>, and dimensions of 89 mm (T) × 120 mm (W) × 3600 mm (L) in size were used in this study. For reinforcement, a 1.3-mm-thick one-way CFRP extruded with epoxy adhesive was used. The epoxy adhesive was also used for timber-reinforcement bonding (Lee *et al.* 2019), and 8-mm-thick steel plates and 12-mm-diameter high-tension bolts were used for the connection.

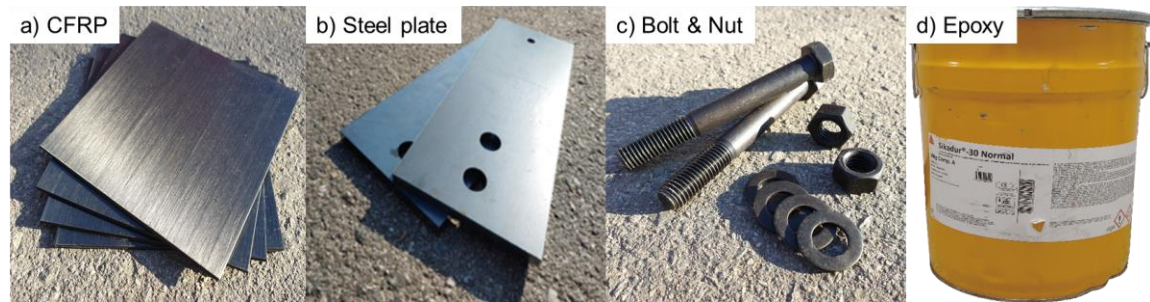


**Fig. 1.** Photographs of the a) CFRP, b) Steel plate, c) Bolt & Nut, and d) Epoxy material used in this study

## Methods

### *Fabrication of the bearing strength specimens*

The control specimens were shaped with 12-mm-diameter bearing points machined onto the cross-section of a timber that was saw-milled into a 120 mm × 38 mm cross-section size and an 84 mm thickness (7D). The experimental specimens were fabricated by reinforcing timbers with one and two CFRP sheets in which the fiber direction of the CFRP was perpendicular to that of the timber. The CFRP1 specimen with one CFRP sheet was reinforced with CFRP at 1.5 times (1.5D) the position of the 12-mm-diameter bolt. The CFRP2 specimen with two CFRP sheets was reinforced with one sheet each at one time (1D) the position of the bolt diameter (Fig. 2). The CFRP1 specimen had a 3.42% reinforcement volume ratio while the CFRP2 specimen had an 6.84% volume ratio. For the reinforced composite timber specimens, 12-mm-wide and 6-mm-deep bearing points (1/2D) were machined onto the cross-section. A total of 24 bearing strength specimens were fabricated, with eight specimens per type.

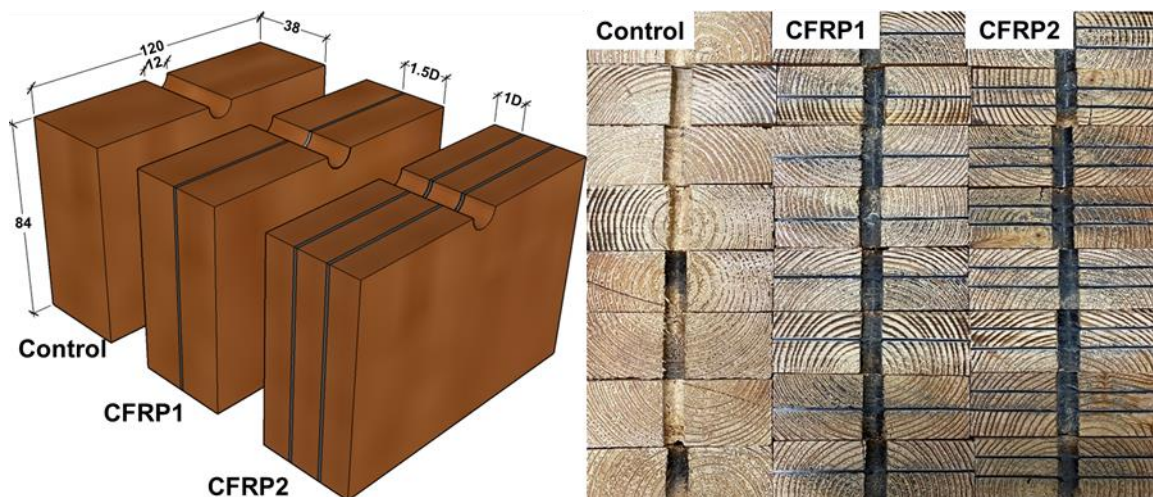


**Fig. 2.** Schematic diagram and photography of the bearing test specimens

### *Fabrication of the tensile shear strength specimens*

The tensile shear test specimen was a steel-plate-insert-type connection in which a 350-mm-long timber was joined by an 8-mm-thick steel plate using 12-mm-diameter bolts. For the control group, a 10-mm-thick slit with a 100 mm or 120 mm length was machined onto the center of the cross-section into which a steel plate was inserted. For the reinforced

specimens, a 13-mm-thick slit with a 100 mm or 120 mm length was machined. For the specimens with a 100-mm-long slit, a 12-mm-diameter hole was drilled at the 5D end distance from the cross-section. For the specimens with a 120-mm-long slit, the hole was drilled at the 7D end distance.

For the composite timber specimens reinforced with CFRP, there were two surfaces in contact with the timber. A steel plate was inserted into these specimens, and two parts where slits were machined onto the timber were reinforced with CFRP with a 6.5% volume ratio. Three types of specimens (types A, B, and C) were fabricated according to the slit position (1D, 1.5D, and 2D of the side member thickness) (Fig. 3). For the type A specimen, a 1.5-mm-thick, 120-cm-long slit was machined onto both sides at the point that was 1D apart parallel from the center slit of the timber to the timber's outer layer. For the type B specimen, a slit with the same size as the type A specimen was machined at the point that was 1.5D apart from the timber's outer layer. For the type C specimen, it was machined at the point that was 2D apart from the center slit to the timber's outer layer. For all the reinforced specimens, the CFRPs were inserted and bonded onto both sides of the center slit and the 1.5-mm-thick slit. As with the control specimens, the steel-plate-insert-type specimens were fabricated in two types of end distance (5D and 7D) according to the bolt diameter. The specimens were reinforced in such a way that the fiber direction of the CFRP was perpendicular to that of the timber. For the attachment of the CRFP to the timber, 300 g/m<sup>2</sup> epoxy adhesive was applied at a 3:1 main agent-hardener ratio, and the attached CRFP was cured under constant compressive pressure for 24 h at room temperature.

Three 12-mm-diameter holes were drilled at the bottom of every specimen's timber to be fixed with a stopper. A total of 40 specimens, with five specimens per type, were fabricated.

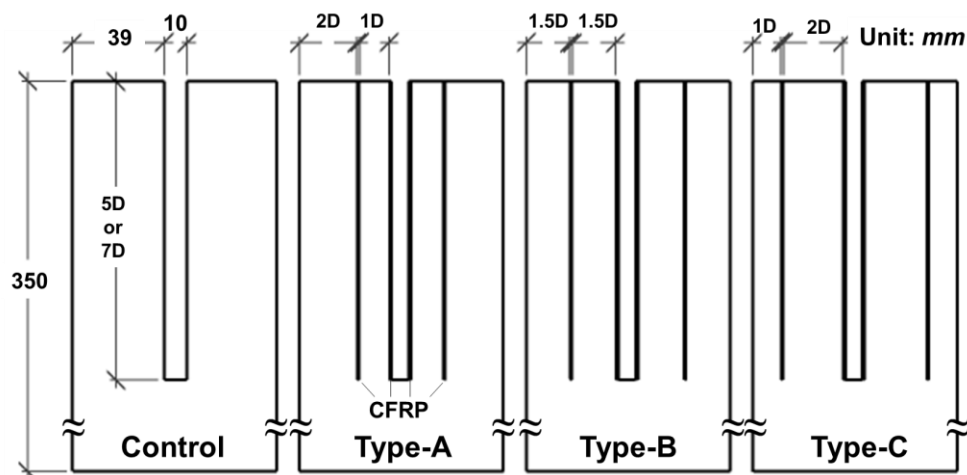


**Fig. 3.** Frontal schematic diagram and photograph of the tensile specimens

#### *Bearing strength test*

The testing for the bearing strength test was conducted on an Instron 4482 universal testing machine (Instron, Norwood, MA, USA). This machine was used to measure both the compressive load and displacement. After positioning the 12-mm-diameter high-tension bolts in the specimen's faster holes, they were installed in such a way that the compressive load would act evenly along the total length of the bolt. The loading rate was set to 3 mm/min. The bearing load was applied in the direction parallel to the fiber until

the maximum load was reached or until the displacement of the timber reached the radius (1/2D) of the faster. The bearing strength was calculated according to Eq. 1,

$$F_b = \frac{P_{max}}{A} \quad (1)$$

where  $F_b$  is the bearing strength (MPa),  $P_{max}$  is the maximum load before the deformation of 1/2D (N), and  $A$  is the bearing cross-section area (mm<sup>2</sup>).

#### Tensile shear strength test

The bottom part of the tensile shear strength specimen was fixed onto the stopper using bolts. The displacement was measured using two 50-mm-diameter displacement meters attached to both sides of the timber via the metal fixture at the top of the inserted steel plate, and the mean value was used. The loading rate was set to 5 mm per minute.

## RESULTS AND DISCUSSION

### Bearing Strength of the Composite Timber

The bearing yield load was determined by moving in parallel the straight-line section in the load deformation curve by 5% of the bolt diameter. The load was measured at the intersection with the load deformation curve, in accordance with the ASTM standard D5764-97a (1997). The mean bearing load of the control timber was measured at 28.1 MPa. The bearing strength-deformation curve in Fig. 3 shows one curve of each samples' representative specimen. The mean bearing yield strengths of the CFRP1 specimen (with one CFRP sheet) and the CFRP2 specimen (with two CFRP sheets) were 25% and 50% higher, respectively, than those of the control specimens (Table 1). Therefore, when the timber was reinforced with CFRP at a 1% volume ratio, the bearing strength improved by 6.25%, on average. The regression analysis results showed a relatively high correlation coefficient of 0.64 (Fig. 4). The control specimens failed due to a crack fracture in the direction of the wood grain after the indentation of the timber by the bolts. The composite timber samples CFRP1 and CFRP2 did not show any crack fracture, and the timber and CFRP samples were indented together to a 1/2D depth.

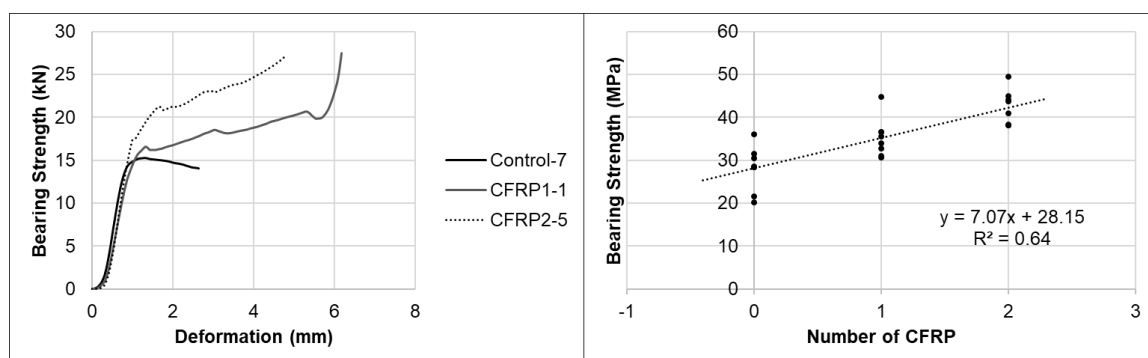


**Fig. 4.** Load-deformation curves of the bearing strength specimen; relationship between the bearing strength and the CFRP reinforcement count

**Table 1.** The 5% Offset Bearing Yield Load on the Reinforced Timber Samples

Specimen	$F_b$ Mean (MPa)	CV(%)*	Ratio of Strength**
Control	28.1	18.2	1.00
CFRP1	35.3	12.8	1.25
CFRP2	42.3	9.7	1.50

\*CV: coefficient of variation, relative standard deviation

\*\* Ratio of  $P_{\text{mean}}$  mean to  $P_{\text{mean}}$  mean 7D control specimen

### Tensile Shear Strength: Load Deformation Curve

Table 2 shows connecting strengths of the tensile shear test specimens, and Fig. 5 shows the load deformation curve graph. The mean maximum connecting strength of the reinforced specimens designed with a 7D end distance was 1.65 to 1.81 times higher than that of the 7D control specimen. This appears to be because the mean maximum connecting strength of the 7D control specimen was 19% higher than that of the 5D control specimen. The maximum connecting strengths of the reinforced specimens fabricated with a 5D end distance were 1.8 to 1.94 times higher than that of the non-reinforced control specimen.

**Table 2.** Comparison of the Shear Strength of the Specimens

Specimen		$P_{\text{max}}$ Mean (kN)	CV*(%)	Ratio of Strength**
5D	Control	29.1	14.0	8.4
	TypeA	56.3	10.4	1.6
	TypeB	52.4	9.5	1.5
	TypeC	56.4	13.3	1.6
7D	Control	34.5	17.0	1.0
	TypeA	56.8	10.5	1.6
	TypeB	62.4	6.9	1.8
	TypeC	62.2	7.8	1.8

\*CV: coefficient of variation

\*\* Ratio of  $P_{\text{mean}}$  mean to  $P_{\text{mean}}$  mean 7D control specimen

Although the 5D type A and C specimens showed similar connecting strength performances, the 5D type C specimen showed better mean initial stiffness and toughness. In the case of the 5D type A specimen, the measured maximum connecting strengths of the specimens with 5D and 7D end distances were similar, and the specimen with a 7D end distance seemed to have better toughness. The type B and C specimens showed maximum connecting strengths that were 10% to 19% higher, and the coefficient of variation was lower in the 7D end distance than in the 5D end distance. All the 7D specimens and the control specimens showed better toughness than the 5D specimens. As connecting strengths of the reinforced 5D specimens were higher than those of the 7D control specimen, when designed with reinforced 5D, the effective pure cross-section area of the flat plate was greater. This will facilitate the aligned, staggered, and reticulated arrangements of the bolts. When a spruce (0.42-0.52), whose specific gravity was similar to that of larch, was reinforced with three sheets of fiberglass (volume ratio: 4.4%), the

maximum load increased 1.33 times (Soltis *et al.* 1998). This is equal to a 13% strength improvement per 1% volume ratio. In this study, the strength increased by 25% per 1% volume ratio, which means that the reinforcement ability of CFRP was better than that of fiberglass.

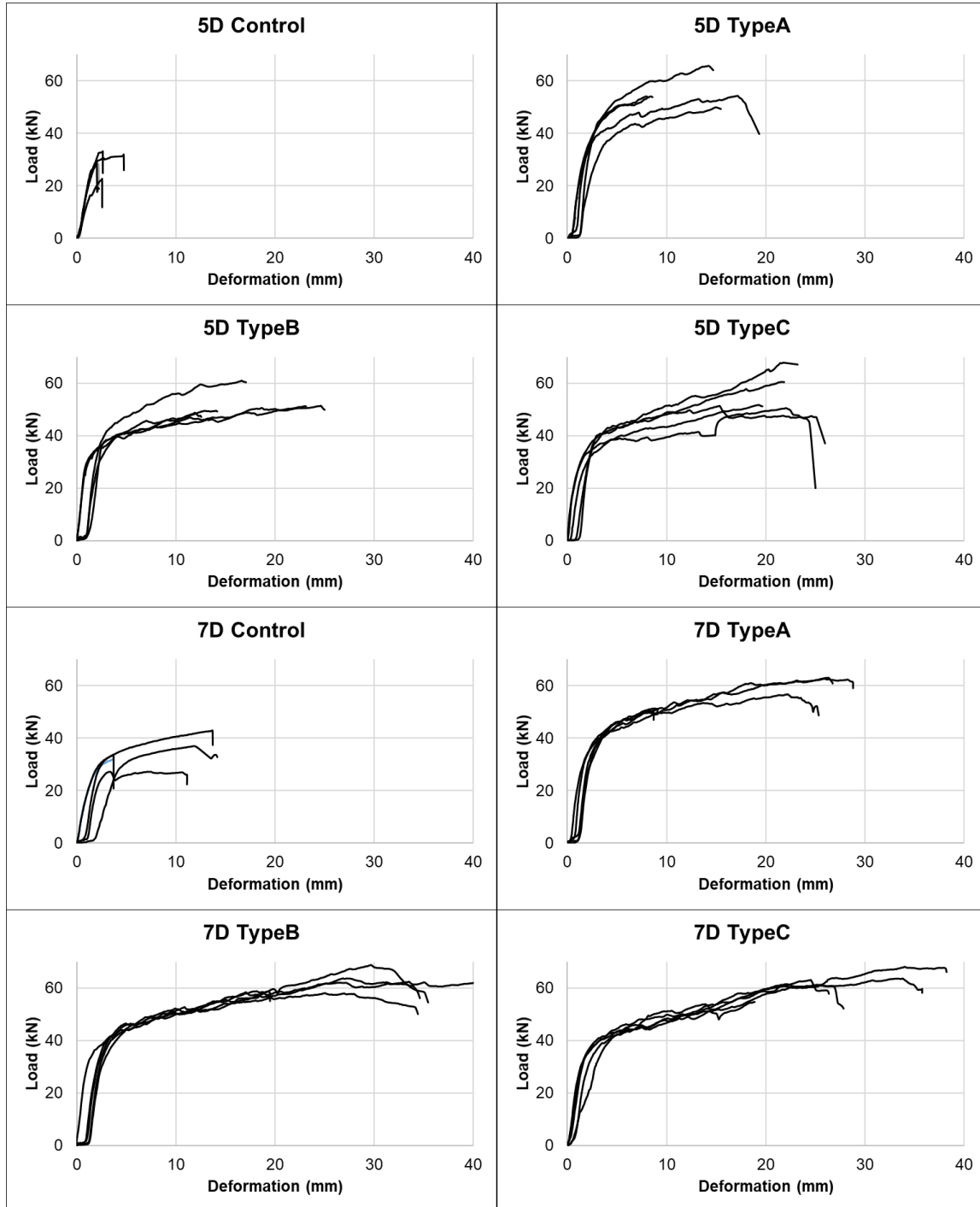


**Fig. 5.** Load-deformation relationship of specimens

### Yield shear strength

The yield shear strength ( $P_y$ ) of the connection was used to calculate the long-term allowable shear strength in the design of the bolt connection structure. The yield shear strength was determined by the load at the intersection of the load deformation curve, with the straight line of the 10% to 20% section of the maximum load moved by 5% of the bolt diameter to the deformation direction (ASTM D5764-97A 1997). The average yield shear strength of the 5D control specimen was 26.6 kN. The average yield shear strengths of the 5D CFRP-reinforced specimens for types A, B, and C were 34.4, 34.4, and 34 kN, which improved by 29%, 29%, and 28%, respectively, compared to the control specimens. The reinforced specimens with a 7D end distance (7D types A, B, and C) also showed average yield shear strengths improved by 24%, 26%, and 27% compared to the control specimens. The CFRP-reinforced 5D specimens showed a 20% average strength improvement compared to the non-reinforced 7D specimens irrespective of the reinforcement position. Although the maximum strength varied by the position of CFRP reinforcement, the yield shear strength did not show significant differences. The coefficients of variation of all the CFRP-reinforced specimens were lower than those of all the control specimens (Table 3).

**Table 3.** Comparison of the Yield Shear Strength of the Specimens

Specimens		$P_y$ Mean(kN)	CV*(%)	Ratio of Strength**
5D	Control	26.6	14.9	0.93
	TypeA	34.4	8.0	1.21
	TypeB	34.4	10.7	1.21
	TypeC	34.0	12.4	1.19
7D	Control	28.9	8.1	1.00
	TypeA	35.2	4.9	1.24
	TypeB	36.0	3.2	1.26
	TypeC	36.1	8.8	1.27

\*CV: coefficient of variation

\*\* Ratio of  $\underline{P}_y$  mean to  $P_y$  mean 7D control specimen

### Failure shape

Figure 6 shows failure shape photographs of the tensile shear test specimens. Most of the specimens appeared to have good bonding performance because the bonding layer between the CFRP and the timber was not separated, and only the wooden part was fractured. The control specimens showed brittle fractures in the cross-sectional direction, as the top part of the bolt was pressured by the rising bolts and steel plate. The bolts of the CFRP-reinforced specimens were not only pressed towards the cross-section; the bolt heads and nuts were also pressed towards the inside of the timber. This characteristic was more conspicuous in the 7D specimens than in the 5D specimens. Cracks occurred in the control and reinforced 5D specimens as the bolts were pressed towards the cross-section, but no fracture of the cross-section was observed in the reinforced 7D specimens. Moreover, in all the specimens, interfacial failure did not occur between the reinforcement CFRP and the timber, indicating good bonding performance between the timber and the CFRP. A higher performance is expected if the pressure of the bolts is minimized by enlarging the washer diameter.

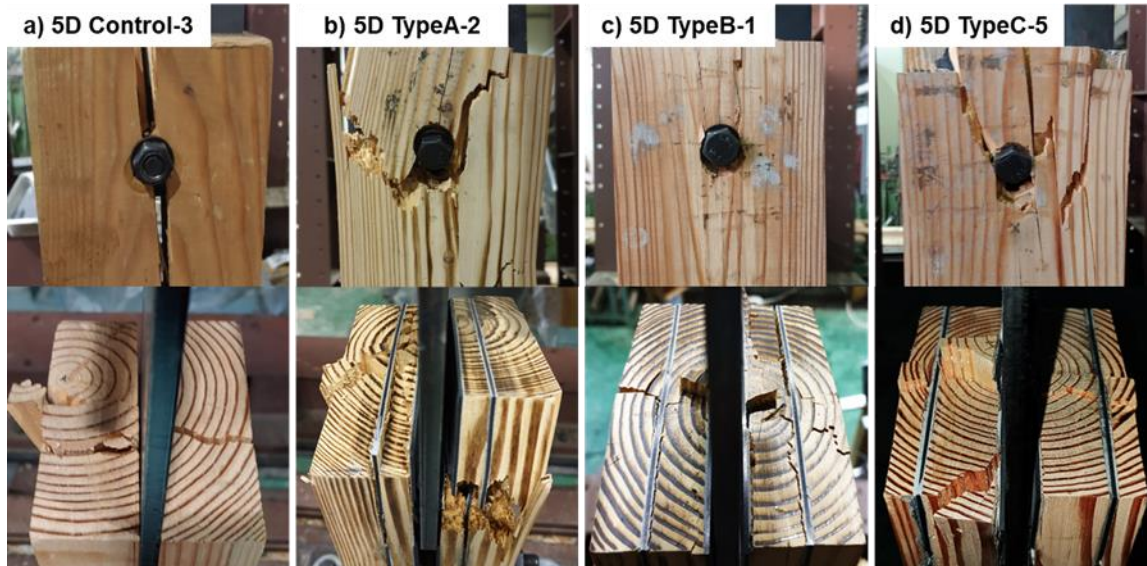


**Fig. 6.** Photographs of the a) 7D Control-1, b) 5D TypeA-2, c) 5D TypeB-1, and d) 7D TypeC-1 specimen failure modes

*Predicted yield shear strength of the CFRP composite timber*

The predicted yield shear strength of single-bolt connections was estimated using the Einstein-Yang-Mills (EYM) theory proposed by Johansen (1949). The EYM theory calculates the yield shear strength by considering the bearing strength, the thickness of the timber, the bolts and steel plate, the fiber direction of the timber, and the failure mode.

**Table 4.** Comparison of the Yield Shear Strength of the Specimens

Mode	Yield Limit Equations		
	NDS	Eurocode 5	KBC (Korea Building Code)
Mode I <sub>s</sub>	$Z = Dl_s kF_s$	$Z = kF_s t_s D$	$Z = \frac{Dt_s kF_s}{K_\theta}$
Model II <sub>s</sub>	$Z = \frac{k_1 Dl_s F_{em}}{(2 + R_e)}$	$Z = kF_s t_s D \left( \sqrt{2 + \frac{4M_y}{kF_s D t_s^2}} - 1 \right)$	$Z = \frac{k_1 D t_s F_{em}}{K_\theta (2 + R_e)}$

$D$  = bolt diameter

$l_s$  = side member fastener bearing length

$F_{em}$  = bearing yield strength of steel plate

$F_s$  = bearing yield strength of timber or reinforced timber

$k$  = bearing strength reinforcement coefficient

$t_s$  = thickness in one of the side timber or reinforced timber

$R_e = F_{em}/F_s$

$$k_1 = -1 + \sqrt{\frac{2(1+R_e)}{R_e} + \frac{2F_y(2+R_e)D^2}{3F_{em}t_s^2}}$$

$$K_\theta = 1 + (\theta_{max}/360^\circ)$$

$\theta_{max}$  = angle of load to the fiber direction of the timber ( $0^\circ \leq \theta \leq 90^\circ$ )

$$M_y = F_y \cdot D^3/6$$

$F_y$  = bolt yield strength

In the study, the failure shapes of Mode I<sub>s</sub> and III<sub>s</sub> for the two-surfaced shear joint presented by Eurocode 5 (1995) and the NDS (1986) were observed (Table 4). Mode I<sub>s</sub> was observed in the non-reinforced control specimens, and Mode III<sub>s</sub> was observed in every reinforced specimen. Mode I<sub>s</sub> occurs when there is no deformation in the main member and bolts and only the side members are indented; thus, the strength of the side member is significantly lower than that of the main member. Mode III<sub>s</sub> occurs when one or more parts of the bolts are bent. The reinforced specimens in this study exhibited the failure shape of Mode III<sub>s</sub> due to the improved bearing strength of the CFRP. The yield shear strength was estimated using the EYM theory of Eurocode 5 (Johansen *et al.* 1949). For the bearing strength of the timber, 28.1 MPa of force was applied. For the reinforced timber, 42.3 MPa of force was applied because one side member was reinforced with two CFRPs. For the high-tension bolts, 900 MPa of force was applied as the yield shear strength.

Table 5 compares the measured yield shear strength ( $P_y$ ) and predicted yield shear strength ( $P_E$ ) by applying the bearing yield strength value obtained in this study. The estimation equation for the predicted yield shear strength varies by country. In this study, the predicted yield shear strengths ( $P_{EEY}$ ) were calculated using the estimation equations proposed by Eurocode 5, NDS, and LBC, and they were then compared with the measured yield shear strengths. For the CFRP-reinforced specimens, the reinforcement coefficient  $k$  (1.065) per 1% CFRP volume ratio was applied based on the cross-section determined by the bearing strength test.

The predicted yield shear strengths proposed by NDS and KBC (Korea Building Code) showed small differences with the yield shear strengths measured in this study, and the result that the predicted yield shear strengths of the CFRP-reinforced specimens were higher than those of the control group was the same. The yield shear strengths predicted using the estimation equation proposed by Eurocode 5 were 0.90 to 1.14 times the measured yield shear strengths, thus showing very similar values. The yield shear strengths predicted using the estimation equations proposed by NDS and KBC were also similar to the measured values (0.90 to 1.17 times the measured values). These results confirmed that the yield shear strength applying the bearing yield strength can also be predicted for the single-bolt steel-plate-insert-type connection of the larch timber.

**Table 5.** Comparison of the Experimental Yield Strength and Revised Yield Strength Proposed by the EYM Theory on Bolted Connection

Specimens		$P_y$ (kN)	$P_E$ (kN)					
			Eurocode 5		NDS		KBC	
			$P_{EEY}$ (kN)	Ratio of Strength	$P_{ENY}$ (kN)	Ratio of Strength	$P_{EKY}$ (kN)	Ratio of Strength
5D	Control	26.6	25.7	0.96	25.65	0.96	25.65	0.96
	TypeA	34.4	38.7	1.12	39.67	1.15	39.68	1.15
	TypeB	34.4	38.7	1.13	39.70	1.16	39.70	1.16
	TypeC	34.0	38.7	1.14	39.68	1.17	39.70	1.17
7D	Control	28.9	25.7	0.90	25.65	0.90	25.65	0.90
	TypeA	35.2	38.7	1.10	39.68	1.13	39.67	1.13
	TypeB	36.0	38.7	1.07	39.70	1.10	39.70	1.10
	TypeC	36.1	38.7	1.07	39.68	1.10	39.70	1.10

## CONCLUSIONS

1. The bearing strength of the larch timber was measured to be 28.1 MPa, and the bearing strength improved by 6.25% when the timber was reinforced with CFRP in a direction perpendicular to the fibers at a 1% volume ratio.
2. The CFRP was found to have a high reinforcement effect as a single reinforcement, despite its low thickness.
3. The results of the tensile shear strength evaluation according to the larch timber-CFRP reinforcement combination showed that with CFRP reinforcement, the mean maximum connecting strengths of the 5D specimens improved by 80% to 94%, and the mean maximum connecting strengths of the 7D specimens improved by 65% to 81%. The mean maximum connecting strengths of the reinforced 5D specimens were all higher than those of the 7D control specimens, and their mean yield strengths were also higher.
4. The failure shape of the control specimens was a brittle fracture of Mode I<sub>s</sub>, and the failure shape of the CFRP-reinforced specimens was a toughness fracture of Mode III<sub>s</sub>.
5. When the measured yield shear strengths were compared with the predicted yield shear strengths, the yield shear strengths predicted using the estimation equation proposed by Eurocode 5 were 0.90 to 1.14 times the measured values, and the yield shear strengths predicted using the estimation equations proposed by NDS and KBC were 0.90 to 1.17 times the measured values. The predictability of yield shear strength was verified, since all predicted yield shear strengths of the specimens were similar to the measured values.

## ACKNOWLEDGEMENTS

This study was conducted as a basic research project supported by the Korea Research Foundation with funding from the Korean Ministry of Education in 2016 (Grant No. R1D1A1B01011163)

## REFERENCES CITED

- ASTM D5764-97a. (1997). "Standard test method for evaluating dowel-bearing strength of wood and wood-base products," American Society for Testing and Materials, West Conshohocken, PA.
- Barber, D. (2017). "Determination of fire resistance ratings for glulam connectors within US high rise timber buildings," *Fire Safety Journal* 91, 579-585. DOI: 10.1016/j.firesaf.2017.04.028
- EN 1995-1-1 (2004). "Eurocode 5 - Design of timber structures," European Committee for Standardization, Brussels, Belgium.
- EN 408 (2011). "Timber structures. Structural timber and glued laminated timber. Determination of some physical and mechanical properties," European Committee for Standardization (CEN), Brussels, Belgium.

- Gečys, T., and Daniūnas, A. (2013). “Experimental investigation of glued laminated timber beam to beam connections filled with cement based filler,” *Procedia Engineering* 57, 320-326. DOI: 10.1016/j.proeng.2013.04.043
- Haller, P., and Wehsener, J. (2000). “Use of technical textiles and densified wood for timber joints,” *Materials for Buildings and Structures* 6, 66-71. DOI: 10.1002/3527606211.ch10
- Johansen, K.W. (1949). “Theory of timber connections,” *Int Assoc. Bridge Struct. Eng.* 9, 249-262.
- Kim, G.-C. (2005). “Study on the improvement of strength capacity for glulam-to-bolt connection,” *Journal of the Korean Wood Science and Technology* 33(6), 31-37.
- Kim, H.-K., Park, C.-Y., and Lee, J.-J. (2008). “Evaluation of the strength properties of glulam connections with inserted steel plates and drift pins,” *Journal of the Korean Wood Science and Technology* 36(2), 29-38. DOI: 10.5658/WOOD.2008.36.2.029
- Le, T. D. H., and Tsai, M.-T. (2019). “Experimental assessment of the fire resistance mechanisms of timber-steel composites,” *Materials* 12(23), 4003. DOI: 10.3390/ma12234003
- Lee, I.-H., Song, Y. J., and Hong, S.-I. (2017). “Evaluation of moment resistance of rigid frame with glued joint,” *Journal of the Korean Wood Science and Technology* 45(1), 28-35. DOI: 10.5658/WOOD.2017.45.1.28
- Lee, I.-H., Song, Y.-J., and Hong, S. I. (2017). “Evaluation of the lateral strength performance of rigid wooden portal frame,” *Journal of the Korean Wood Science and Technology* 45(5), 535-543. DOI: 10.5658/WOOD.2017.45.1.28
- Lee, I.-H., Pack, J.-H., Song, D.-B., and Hong, S.-I. (2018). “Longitudinal bonding strength performance evaluation of larch lumber,” *Journal of the Korean Wood Science and Technology* 46(1), 85-92. DOI: 10.5658/WOOD.2018.46.1.85
- Lee, I.-H., Song, Y.-J., Song, D.-B., and Hong, S.-I. (2019). “Results of delamination tests of FRP-and steel-plate-reinforced larch composite timber,” *Journal of the Korean Wood Science and Technology* 47(5), 655-662. DOI: 10.5658/WOOD.2019.47.5.655
- NDS (1986). “National design specifications for wood construction,” American Wood Council, Washington, D.C.
- Soltis, L. A., Ross, R. J., and Windorski, D. F. (1998). “Fiberglass-reinforced bolted wood connections,” *Forest Products Journal* 48(9), 63-67.
- Song, Y.-J., Lee, I.-H., and Hong, S.-I. (2019). “An evaluation of strength performance of the edge connections between cross-laminated timber panels reinforced with glass fiber-reinforced plastic,” *BioResources* 14(4), 7719-7733. DOI: 10.15376/biores.14.4.7719-7733
- Xu, B.-H., Bouchair, A., Taazount, M., and Vega, E. J. (2009). “Numerical and experimental analyses of multiple-dowel steel-to-timber joints in tension perpendicular to grain,” *Engineering Structures* 31(10), 2357-2367. DOI: 10.1016/j.engstruct.2009.05.013

Article submitted: July 30, 2020; Peer review completed: November 28, 2020; Revisions accepted: May 18, 2021; Published: May 27, 2021.

DOI: 10.15376/biores.16.3.5106-5117